Expression and activation of the farnesoid X receptor in the vasculature

David Bishop-Bailey*†, Desmond T. Walsh‡, and Timothy D. Warner*

*Cardiac, Vascular, and Inflammation Research, William Harvey Research Institute, Barts and the London, Queen Mary University of London, Charterhouse Square, London EC1M 6BQ, United Kingdom; and ‡Department of Neuroinflammation, Division of Neuroscience and Psychological Medicine, Faculty of Medicine, Imperial College of Science, Technology and Medicine, Charing Cross Hospital, Fulham Palace Road, London W6 8RF, United Kingdom

The farnesoid X receptor/bile acid receptor (FXR) is a recently discovered member of the nuclear hormone superfamily. FXR ligands have been proposed as targets in cardiovascular disease, regulating cholesterol metabolism and bile acid transport and metabolism in the liver and gastrointestinal tract. When we used a human cardiovascular tissue array, we found that FXR is expressed in a variety of normal and pathological human tissue. Particularly high levels of FXR were found in the vasculature and in a number of different metastatic cancers, as well as the previously identified target tissues of the liver, small intestine, and kidney. In vitro, FXR is present in rat and human vascular smooth muscle cells. When treated with a range of FXR ligands, vascular smooth muscle cells undergo apoptosis in a manner that correlates with the ligands' ability to activate FXR. Furthermore, FXR activators induce mRNA for the FXR target genes, phospholipid transfer protein, and the small heterodimer partner. FXR therefore is a functional protein in the vasculature that may provide a direct target for the treatment of proliferative and dyslipidaemic diseases.

Hypercholesterolemia is a major risk factor for atherosclerosis and related vascular diseases. The farnesoid X receptor (FXR; NR1H4) is a member of the steroid superfamily of nuclear receptors/transcription factors that binds and acts as a heterodimer with retinoid X receptors (RXR; ref. 1). FXR was originally identified as a receptor activated by high levels of the isoprenoid cholesterol synthesis intermediate farnesol, and the sesquiterprenoid insect mediator juvenile hormone III (JHIII; ref. 1). However, FXR was subsequently characterized as a bile acid receptor (2, 3), correlating to the high levels of mRNA for FXR that are found in the liver and gastrointestinal tract (1), sites at which bile acids are present and known to act. Bile acids, the major product of cholesterol metabolism, regulate circulating cholesterol through multiple FXR-dependant pathways. Activation of FXR causes both feedback inhibition of cholesterol 7α-hydroxylase (CYP7A1), the rate-limiting enzyme in bile acid biosynthesis from cholesterol, and activation of intestinal bile acid-binding protein (4). Interestingly, $FXR^{-/-}$ knockout mice (5) display a proatherogenic lipid profile, having increased circulating total cholesterol, triglycerides, phospholipids, and cholesterol esters, decreased hepatic scavenger receptor B1, and an increase in apolipoprotein B1. Although bile acid sequestrants are used to treat hypercholesterolemia, bile acids such as chenodeoxycholic acid (CDCA) lower circulating cholesterol in some patients (6).

High levels of mRNA for FXR are also found in the kidney and adrenal gland, areas of the body not classically considered as being bile acid targets (1), whereas low levels of mRNA for FXR are present in a variety of tissues, including heart, ovary, thymus, eye, spleen, and testes (7, 8). The roles of FXR in these tissues are not known, nor indeed is the potential of bile acids to act as its ligands. Furthermore, the expression of FXR protein, especially in human tissue, is poorly understood. In addition, splice variants of FXR have recently been identified that have different pharmacology (7) and/or different expression patterns (8). The roles of these splice variants in man are also unknown.

Synthetic FXR ligands have been identified, including GW4064 (9), fexaramine (10), and a series of 1,1-bisphosphonate esters (11), including Apomine (SR45023A). The 1,1-bisphosphonate esters, which may be antineoplastic drugs (12), induce apoptosis in a number of cancer cell lines, and are hypocholesterolemic in cynomolgus monkeys (11).

Here we report FXR protein expression in man, with the unexpected finding that FXR is highly expressed in the vascular smooth muscle of normal and atherosclerotic blood vessels. Furthermore, in vitro FXR is a functional vascular smooth muscle cell receptor regulating both proliferation and the levels of the target genes small heterodimer partner (SHP) and the phospholipid transfer protein (PLTP), an important regulator of reverse cholesterol transport.

Materials and Methods

Immunohistochemical (IHC) Analysis. LandMark LD Cardiovascular Tissue arrays were purchased from Ambion. IHC was performed by standard techniques as described (13). Anti-FXR antibodies [sc-1204 goat anti-FXR (C-terminal), and its corresponding blocking peptide; and sc-13063, rabbit anti-FXR (N-terminal)] were purchased from Santa Cruz Biotechnology and used at a dilution of 1:50. Blocking peptide for sc-1204, was used in some experiments in 10-fold excess after a 1-h preincubation with primary antibody.

Cell Culture. WKY3m-22 rat aortic smooth muscle cells (RASMC), primary RASMC, and human primary saphenous vein smooth muscle cells (hSVSMC) were grown and maintained as described (14, 15). Primary cells were used between passages 2 and 5. CACO and HepG2 cells were from European Collection of Cell Cultures, and MCF-7 cells were from the American Type Culture Collection. In all experiments, cells were serum-starved for 24 h before use.

Immunoflorescence for FXR and RXR. Confocal immunofluorescence was as described (14), using goat anti-FXR sc-1204 (1:50) and blocking peptide where indicated (10-fold excess; 1-h preincubation), or rabbit anti-RXR (1:50 dilution; Santa Cruz Biotechnology; sc-774).

RT-PCR for FXR, SHP, and PLTP. Total RNA was extracted from the cells by TRIzol reagent (Invitrogen). RT-PCR was performed by using standard techniques. For human FXR (362-bp product), primers were 5′-GCAGCCTGAAGAGTGGTACTCTC-3′ and

---

5′-CATTCAGCCAACATTCCCATCTC-3′ (Eric Niesor, ILEX, Geneva, personal communication); for rat FXR (200-bp product), primers were 5′-CAGCAGACCCTCCTGGATTA-3′ and 5′-TCTTCGTGGTCCAGTGTCTG-3′; for rat PLTP (378-bp product) primers were 5′-GTGGGCAAGAGGTGCT-AAGA-3′ and 5′-GTCACTGTTGGGGATGACCT-3′; for rat SHP (213-bp product) primers were 5′-CCTTGGATGTC-CTAGGCAAG-3′ and 5′-CACCACTGTTGGGGTTCCTCT-3′.

Rat FXR, PLTP, and SHP primers were designed in Primer3 (http://www-genome.wi.mit.edu/cgi-bin/primer/primer3_www.cgi). Rat GAPDH was chosen as a control (14). Initial denaturing was done at 94°C for 3 min followed by 35–40 cycles (human FXR), 35 cycles (rat PLTP or rat SHP), or 30 cycles (GAPDH, both cell types) followed by 10 min at 72°C. For human FXR, each cycle consisted of 30 s at 94°C, 30 s at 57°C, and 30 s at 72°C. For rat SHP, each cycle consisted of 30 s at 94°C, 30 s at 59°C, and 30 s at 72°C. For rat PLTP, each cycle consisted of 35 s at 94°C, 35 s at 58°C, and 45 s at 72°C. PCR products were size fractionated with a 2% agarose gel and the bands visualized with ethidium bromide. Each PCR resulted in a single band at the appropriate base pair size. In parallel reactions where Moloney murine leukemia virus reverse transcriptase was omitted, no bands were visible (data not shown). For quantification, bands were analyzed by using UTHSCSA IMAGE TOOL V.3. For SHP and PLTP measurements, RASMC were incubated with vehicle (0.1% ethanol; 0.05% DMSO), guggulsterone [30 μM; 4,17 (20)-(trans)-pregnadien-3, 16-dione; Steraloids, Newport, RI], SR42023A (10 μM), or CDCA (30 μM), alone or in combination with guggulsterone for 6 h in complete DMEM containing 10% FCS. Guggulsterone was given as 1 h before the addition of the FXR ligands.

Western Blot Analysis for FXR. Protein extraction and Western blot analysis were as described (14), using the rabbit anti-FXR antibody (1:100; Santa Cruz Biotechnology, sc-13063). As a positive control, HepG2 cells grown in 10-cm dishes were transfected with the rat FXR expression plasmid, pSV-FXR, or empty pcDNA3.1 (Invitrogen); and 24-h incubation with 0.5 μg of each plasmid by using Effectene (Qiagen, Crawley, U.K.; according to the manufacturer's recommended protocol).

Measurement of Vascular Smooth Muscle Death. Cell viability was measured by the 3-(4,5-dimethylthiazol-2-yl)-2,5-diphenyl tetra-zolium bromide (MTT) assay (12). In serum-free media, cells were treated with test compounds or vehicles (0.1% ethanol or 0.5% DMSO; concentrations that had no significant effects) for 48 h. Apoptosis was measured by cytoplasmic histone-associated DNA fragment detection ELISA (Roche Diagnostics) or by nuclear morphology after Hoechst staining (16) after 24-h treatment with compounds.
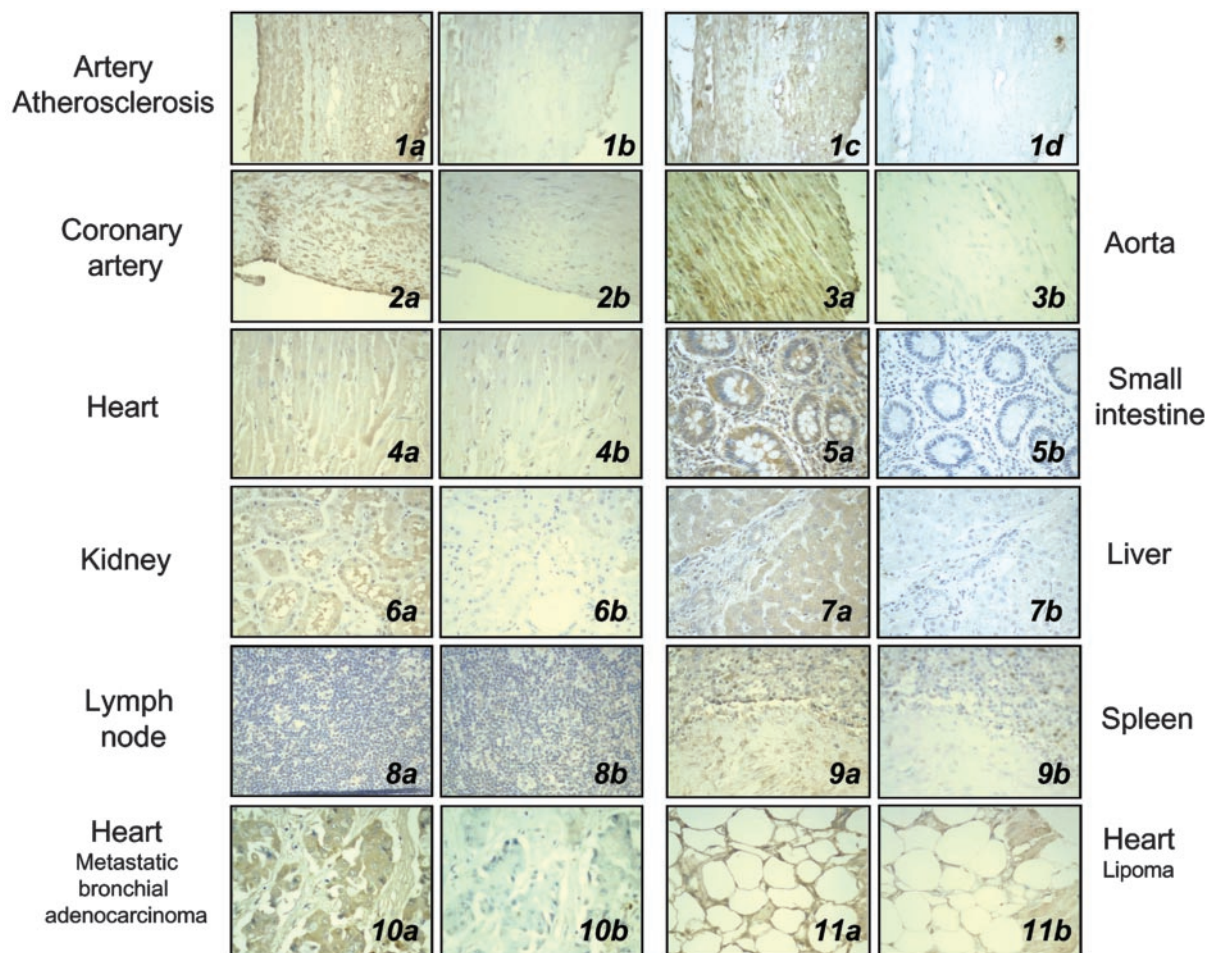
Fig. 1. Immunohistochemical analysis of FXR expression in human tissue array. (*a* and *c*) FXR immunohistochemisty. (*b* and *d*) Control staining (blocking peptide in *1b*, *2*, *4*, *6*, and *8–11*; or primary antibody omitted in *1d*, *3*, *5*, and *7*). The four pictures in series *1* are of the same atherosclerotic artery, confirming the reproducible expression pattern for FXR with either antibodies raised against the C terminus (*a* and *b*) or N terminus (*c* and *d*) of FXR. Compared to control, positive immunoreactive protein (brown immunoperoxidase) was found in atherosclerotic arteries, the coronary artery, and aorta, heart, small intestine, kidney, liver, spleen, and metastatic bronchial adenocarcinoma, and metastatic lipoma, but not the lymph node. All magnifications are ×200.

Results

Cardiovascular Tissue Array Analysis of FXR Expression. FXR was present in the vascular smooth muscle of the coronary artery (Fig. 1 *2*) and aorta (Fig. 1 *3*), and within atherosclerotic lesions (Fig. 1 *1*) $n = 11$ (Fig. 7, which is published as supporting information on the PNAS web site). Lower levels of FXR were found in cardiac muscle (Fig. 1 *4*) and in sections from hypertrophic heart, heart failure, and myocardial infarction (data not shown). Furthermore, we confirm the positive expression of FXR in the small intestine (Fig. 1 *5*), kidneys (Fig. 1 *6*), liver (Fig. 1 *7*), and adrenal gland (Fig. 7) and lack of FXR expression in lymph nodes (Fig. 1 *8*). Interestingly, we also found low levels of FXR in the spleen (Fig. 1 *9*) and very high levels of FXR staining in the heart containing metastatic bronchial adenocarcinoma (Fig. 1 *10*), lipoma (Fig. 1 *11*), metastatic Ewing's sarcoma, and malignant lymphocytic lymphoma (Fig. 7).

Because antibodies had not been characterized for immunohistochemical analysis of FXR, staining patterns were determined by using primary polyclonal antibodies raised against peptide sequences corresponding to regions in either the N or C terminus of FXR. Fig. 1 *1a* and *1c* show that the patterns of FXR expression were virtually identical with either N- or C-terminal antibodies (Fig. 1 *1a* C terminus antibody, and *1c* N terminus antibody), and levels of positive staining were significantly reduced by the use of blocking peptide, or were absent if primary antibody was excluded (Fig. 1 *1b* and *1d*).

FXR Is Expressed in Vascular Smooth Muscle Cells *in Vitro*. FXR expression was determined in vascular smooth muscle cells by confocal immunofluorescence (Fig. 2*A*), RT-PCR (Fig. 2*B*), and Western blot analysis (Fig. 2*C*). In RASMC, FXR, like RXR, had a predominantly nuclear localization, with weak staining throughout the cytoplasm. FXR mRNA measured by RT-PCR was present as a 362-bp band in the FXR-positive control cells lines, CACO and HepG2 (Fig. 2*B*). It was also present in three separate cultures of hSVSMC (1–3), and in the breast cancer cell line MCF-7. RT-PCR for FXR in RASMC indicated the presence of a single 200-bp band corresponding to the predicted size of FXR (data not shown). FXR protein (as a band of ≈ 55 kDa) was present in HepG2 (Fig. 2*C*), and specifically increased when cells were transfected to overexpress FXR (1). Low levels of FXR protein were detected in WKY 3m-22 and primary RASMC, and were present as a doublet in hSVSMC (from three separate patient sources).

FXR/RXR Agonists Induce Vascular Smooth Muscle Cell Death by Apoptosis. The RXR ligand 9-*cis* retinoic acid (9cRA), up to 30 μM, induced RASMC death in a concentration-dependent manner (Fig. 3*A*). The FXR activator farnesol, up to 300 μM, had no direct effect on RASMC viability, but did synergize with 9cRA to induce cell death (Fig. 3*A*). Structural analogues of farnesol involved in the mevalonic acid pathway, squalene, mevalonic acid, and 25-HO-cholesterol, all at 300 μM, had no effect on the cell death induced by 9cRA (Fig. 3*B*). Importantly, these analogues, unlike farnesol, do not activate FXR. Farnesol is an extremely weak FXR activator, so we tested a range of FXR ligands/activators. JH III, the bile acids deoxycholic acid (DCA) and CDCA, and the synthetic FXR ligands SR9213, SR45023A (Apomine), and GW4064 (data not shown) all induced RASMC cell death in concentration-dependent manners, correlating with their ability to activate FXR (Fig. 3*C*). Similar to farnesol, when tested against a concentration range of 9cRA, all of the FXR ligands synergized to induce RASMC death (Fig. 3*D*). RASMC death induced by SR45023A or SR9213 was characterized as apoptosis by the induction of nuclear condensation, (Fig. 4 *Upper*), and by the concentration-dependent appearance of cytoplasmic histone-associated DNA fragments (Fig. 4 *Lower*).
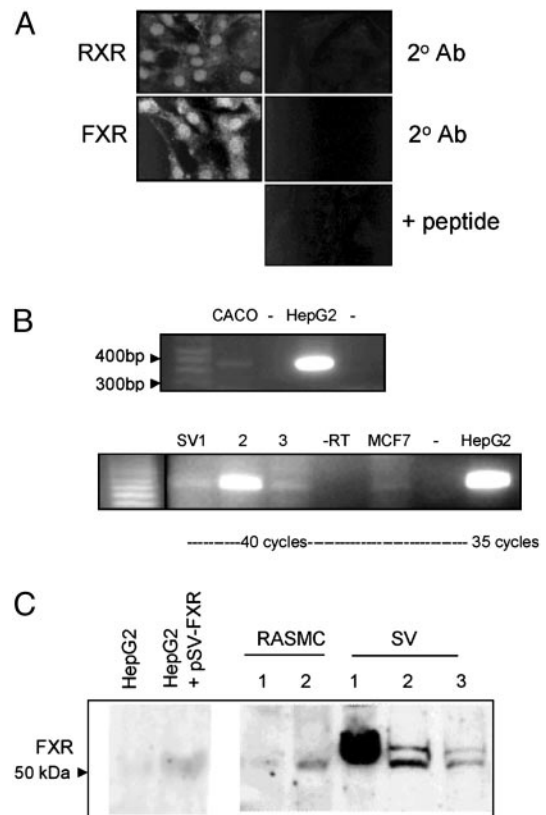

Fig. 2. FXR is expressed in vascular smooth muscle cells. (*A*) Immunofluorescence for FXR and RXR in RASMC. The 2°Ab is negative control for when primary antibody was omitted; + peptide is immunofloresence of FXR, performed with primary antibody preabsorbed with blocking peptide. (*B*) RT-PCR for hFXR. (*Upper*) FXR as a band at 362 bp in the positive controls CACO and HepG2; −, RT-PCR when reverse transcriptase was omitted. (*Lower*) RT-PCR for hFXR on hSVSMC (SV1–3) from three patients, −RT where reverse transcriptase was omitted (for SV3), MCF-7 cells (−RT), and in the positive control HepG2 cells. (*C*) Western blot analysis for FXR in HepG2 cell (transfected empty vector), HepG2 cells transfected with rat FXR (24 h), RASMC (1, WKY3m-22; 2, primary RASMC), and hSVSMC (SV1–3 from three patients). Note that SV sources 1–3 from RT-PCR do not correspond to SV 1–3 in Western blot.

Similarly, JHIII or farnesol (data not shown) synergized with 9cRA to induce cytoplasmic histone-associated DNA fragments (fold enrichment from control; JHIII, 300 μM, 2.0 ± 0.5; 9cRA, 10 μM, 1.0 ± 0.1 fold enrichment; JHIII plus 9cRA, 5.6 ± 0.1; $n = 3$ for each; 24 h)

Similar results were found in hSVSMC, in which the weak FXR activator JH III had little effect alone but synergized with 9cRA to induce cell death (Fig. 5*A*), whereas the potent synthetic ligands SR45023A and SR9213 induced cell death alone (Fig. 5*B*). In hSVSMC, as in RASMC, 9cRA also synergized with SR45023A and SR9213 (data not shown) to induce cell death (control, 100% viable cells; SR45023A 3 μM, 43 ± 7%; 9cRA, 3 μM, 92 ± 8%; SR45023A plus 9cRA, 8 ± 3%; $n = 9$ from three patients). Over 24 h, guggulsterone (refs. 17–19; 100 μM) alone induced hSVSMC death (59 ± 3% viable cells compared to control). Guggulsterone at this concentration had an additive effect on cell death induced by a submaximal concentration of SR45023A (10 μM alone, 71 ± 2% viable cells; +100 μM guggulsterone, 25 ± 2%), but inhibited the cell death caused by a maximum concentration of SR45023A (30 μM alone, 1 ± 1% viable cells; +100 μM guggulsterone, 28 ± 1%; all data, $n = 6$ from two patients sources).
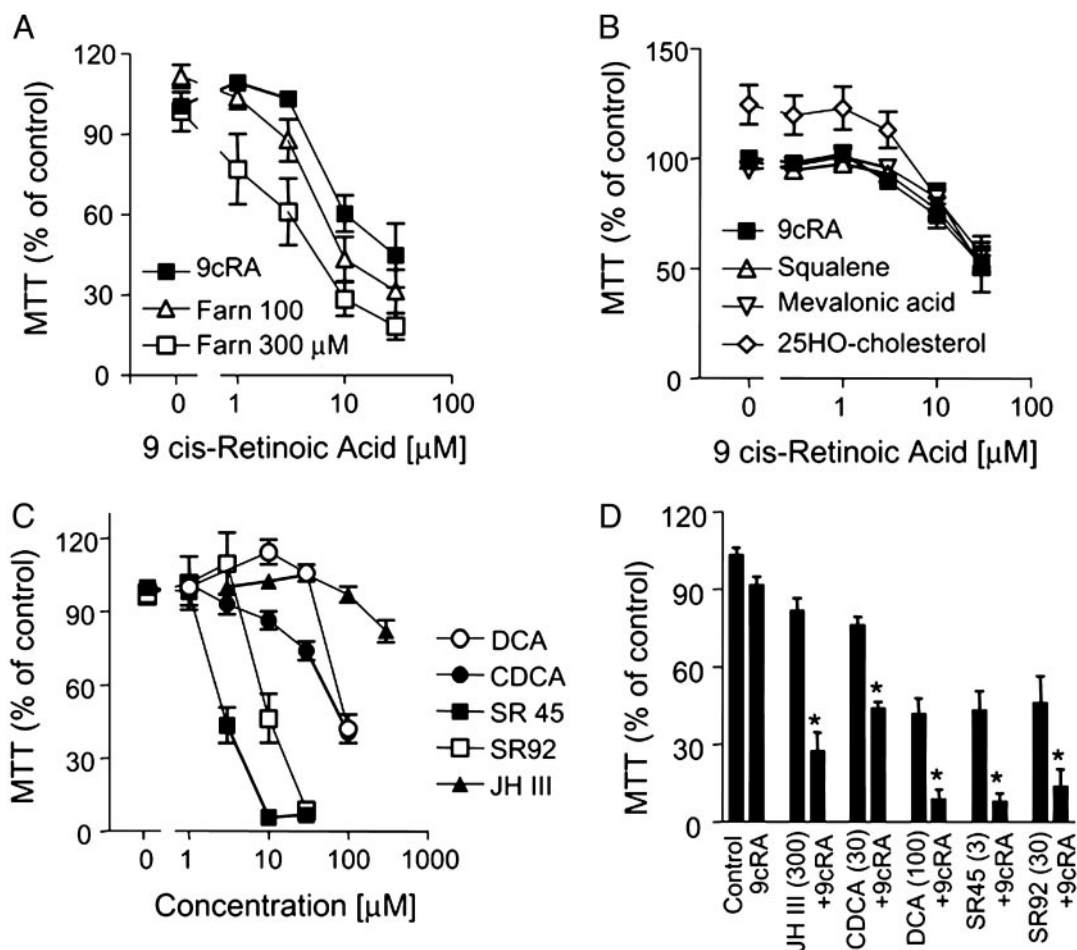
Bishop-Bailey *et al.*

Fig. 3. FXR activators induce RASMC death. Data represent viability as percentage of control (i.e., untreated or vehicle-treated cells = 100%). (*A*) The effect of farnesol (Farn), 100 or 300 μM, on the cell death induced by the RXR ligand 9cRA. (*B*) Effect of squalene, mevalonic acid, or 25-HO-cholesterol, all 300 μM, on the cell death induced by the RXR ligand 9cRA. (*C*) Concentration-dependent effects on RASMC viability of FXR ligands; SR42, SR42023A; SR92, SR9213; DCA, deoxycholic acid. (*D*) Synergistic effects of 9cRA and FXR ligands on RASMC viability. The data represent $n = 12$ from four separate experiments. Asterisks denote $P < 0.05$ between control or ligand treatment alone and in the presence of 9cRA (by paired t test).

Activators Regulate FXR Target Gene Expression in Vascular Smooth Muscle Cells. The FXR target genes SHP and PLTP were measured by semiquantitative RT-PCR (Fig. 6). Low levels of mRNA for SHP and PLTP were observed in RASMCs. The potent synthetic FXR ligand SR45023A (10 μM) alone, but not CDCA (30 μM) induced SHP (Fig. 6*A*) and PLTP (Fig. 6*B*) mRNA. Interestingly, guggulsterone alone inhibited the basal expression of SHP and PLTP, had no effect on the induction caused by the potent FXR ligand SR45023A, and synergized with CDCA to induce both SHP and PLTP (Fig. 6).

Discussion

Vascular smooth muscle cells not only play important structural and homeostatic roles in the blood vessel, but once activated can proliferate and secrete a wide variety of mediators that regulate many aspects of vascular disease progression (20). Here we show that FXR is expressed in vascular smooth muscle *in vitro* and in the vascular wall of normal and atherosclerotic human vessels. Immunoreactivity for FXR was also displayed on the lumen of some large vascular tissue sections (Fig. 1 *1a* and *2a*), suggesting an endothelial expression of FXR; although whether endothelial cells do contain FXR has yet to be confirmed. Similarly, whether FXR is present in monocyte/macrophages within vascular lesions is also yet to be determined. However, when previously

investigated in THP-1 cells, mRNA for FXR was not found under any condition tested (21).

FXR activators induce smooth muscle cell apoptosis in a manner that correlates with their ability to activate FXR (1–3, 11). Furthermore, chemically distinct FXR activators all synergize with the RXR ligand 9cRA to induce SMC death. SR45023A also induced expression of the FXR target genes SHP and PLTP. SHP (NROB2; ref. 22) is an atypical orphan nuclear receptor that lacks a DNA-binding domain but contains a putative ligand-binding domain. SHP is a corepressor to a variety of nuclear receptors including the liver X receptor (23) and the glucocorticoid receptor (24). PLTP is a secreted protein that regulates the reverse cholesterol transport and the size and composition of the vascular protective HDL (25). These findings strongly suggest that FXR, like its related nuclear rector family members peroxisome proliferator-activated receptors (26) and liver X receptor (27), is a pleiotrophic target that regulates vascular smooth muscle proliferation, the function of other nuclear receptors, and lipid metabolism.

FXR was present in all VSMCs examined *in vitro* and *in vivo*, findings that were also consistent between rat and human medial vascular smooth muscle cells, as well as rat intimal/developmental vascular smooth muscle cells (ref. 14 and Fig. 8, which is published as supporting information on the PNAS web site). Under culture conditions, primary cells contained higher
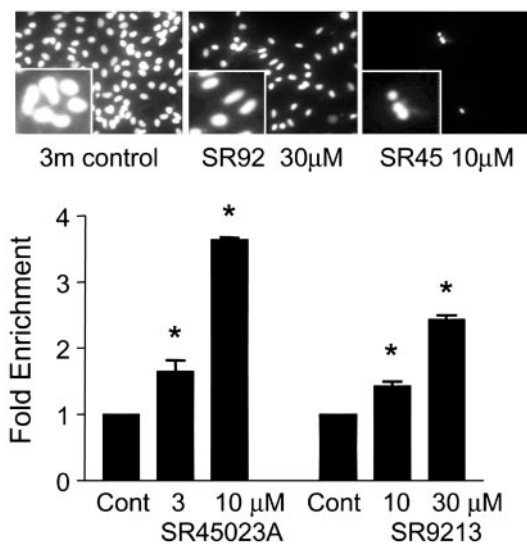
Fig. 4. FXR activators induce RASMC apoptosis. (*Upper*) Hoechst staining of the nuclear morphology of cells (×400 magnification). (*Lower*) Fold enrichment from control (vehicle) of cytoplasmic histone-associated DNA of cells treated with SR9213, or SR42023A. Data are from three separate experiments. Asterisk denotes $P < 0.05$ between control and treated groups, determined by one sample t test.

levels of FXR than the cell lines. Western blot for FXR in hSVSMC revealed a doublet; further investigation is required to determine whether this represents splice variants of FXR or a form of posttranslational modification.
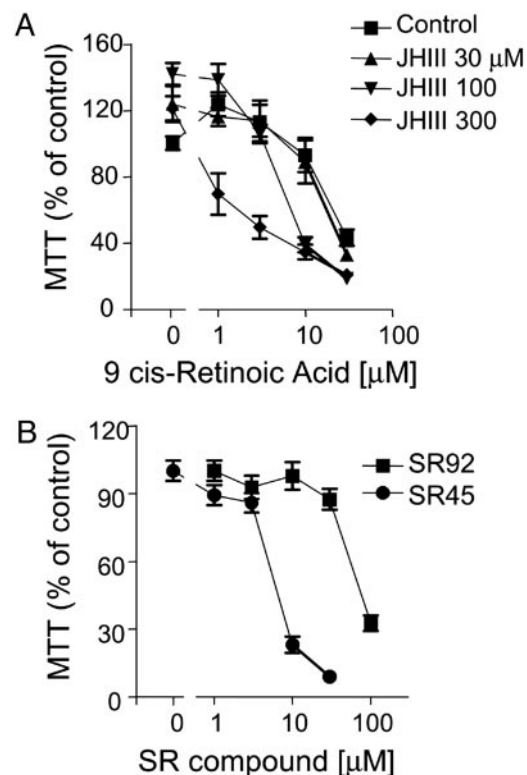

Fig. 5. FXR ligands induce hSVSMC death. Images represent viability as % of control (i.e., untreated or vehicle-treated cells = 100%). (*A*) Effect of JHIII on the cell death induced by the RXR ligand 9cRA. (*B*) Effect of the synthetic FXR ligands SR42023A and SR9213 on hSVSMC viability. Data are $n = 6$ using tissue from two patients.
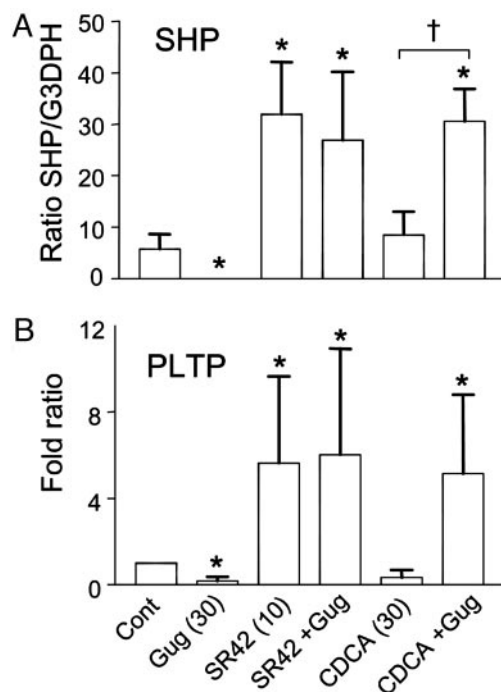

Fig. 6. FXR ligands induce SHP and PLTP mRNA in RASMC. Semiquantitative RT-PCR showing the relative ratio of SHP mRNA (ratio) (*A*) or PLTP mRNA (fold ratio compared to control) (*B*) to constitutive GAPDH mRNA in RASMCs treated with vehicle (Control), guggulsterone (Gug), SR42023A (SR42), and CDCA, alone or in combination with guggulsterone (+G) ($n = 4$, for each). SHP was not normalized to fold ratio, because in one experiment no SHP was detected in control treated cells. Asterisk denotes significance $P < 0.05$ between control and treatment groups, determined by one-way ANOVA for SHP and one-sample t test for PLTP. Dagger denotes significance $P < 0.05$ between FXR ligand alone and in the presence of guggulsterone, determined by paired t test for SHP.

The bile acid CDCA was a weak inducer of apoptosis, and was without effect alone on the FXR target genes SHP and PLTP. We found weak expression of FXR in the heart and spleen, and clear evidence for the well documented expression of FXR in isoprenogenic tissue such as the adrenal glands. Although considerable levels of bile salts do circulate, albeit bound to albumin, our findings clearly raise the question of whether there are other endogenous ligand(s) that activate FXR in these tissues. This appears likely, because androsterone induces FXR reporter gene responses in HepG2 cells to a similar extent as CDCA (28).

Guggulsterone has been described as a FXR antagonist (17), although it is clear from recent findings that it acts as a selective modulator (18, 19), acting as both an antagonist in coactivator assays and an enhancer of the transcription of the FXR target gene, bile salt export pump (18). Guggulsterone alone reduced the basal levels of mRNA for SHP or PLTP, but had no effect on the induction of SHP or PLTP by SR42023A. Guggulsterone did, however, synergize with CDCA to induce the expression of SHP and PLTP. Overall, these findings are consistent with the emerging consensus on the mode of nuclear receptors actions: that agents that bind have a variety of actions through the initiation of different individual coactivator, corepressor protein–protein interactions (29). Our findings support the proposal that guggulsterone is a selective FXR modulator.

Synthetic FXR ligands are inhibitors of the growth of a number of primary and tumor cell lines (12). As in vascular smooth muscle, FXR ligands induce apoptosis, associated with cytoplasmic DNA–chromatin complexes, DNA laddering, and caspase-3 activation in a variety of cancer cells (11). The initial

Bishop-Bailey *et al.*

targets for FXR-induced apoptosis have yet to be identified, although FXR activation similar to related steroid receptors, such as the glucocorticoid receptors and peroxisome proliferator-activated receptors, induces apoptosis in susceptible cell lines. Interestingly, in the tissue array analysis, we found some of the strongest positive staining for FXR in metastatic tumors in the heart, from bronchial adenocarcinoma and lymphoma, although lower levels were found in metastatic Ewing's sarcoma and malignant lymphocytic lymphoma (Fig. 7). These findings suggest that, like many of its related nuclear receptors, FXR is aberrantly expressed in a number of human tumors and is a bona fide antiproliferative therapeutic target.

Our results clearly show that FXR is expressed in a variety of "nonclassical" bile acid target tissues. What the full *in vivo* role of FXR is, and whether bile acids are endogenous ligands for the FXR in all these tissues remains to be seen. Bile acids do have a wide range of effects; CDCA dissolves cholesterol gallstones and is used for the management of cerebrotendinous xantho-matosis, hypertriglyceremia, congenital liver diseases, rheumatoid arthritis, and constipation (30). It is tempting to speculate that some of these effects are mediated by FXR. FXR is expressed in the vasculature and vascular smooth muscle cells *in vitro*. FXR ligands have been proposed as possible drugs to target cardiovascular disease by affecting lipid metabolism in the liver. Here we show that, more fundamentally, FXR is a direct target in the vasculature. Furthermore, our findings show that, like many of its related nuclear family members, FXR has potentially a far greater number of roles throughout the body than originally thought.

1. Forman, B. M., Goode, E., Chen, J., Oro, A. E., Bradley, D. J., Perlmann, T., Noonan, D. J., Burka, L. T., McMorris, T., Lamph, W. W., *et al.* (1995) *Cell* **81,** 687–693.
2. Makishima, M., Okamoto, A. Y., Repa, J. J., Tu, H., Learned, R. M., Luk, A., Hull, M. V., Lustig, K. D., Mangelsdorf, D. J. & Shan, B. (1999) *Science* **284,** 1362–1365.
3. Parks, D. J., Blanchard, S. G., Bledsoe, R. K., Chandra, G., Consler, T. G., Kliewer, S. A., Stimmel, J. B., Willson, T. M., *et al.* (1999) *Science* **284,** 1365–1368.
4. Chiang, J. Y. (2002) *Endocr. Rev.* **4,** 443–463.
5. Sinal, C. J., Tohkin, M., Miyata, M., Ward, J. M., Lambert, G. & Gonzalez, F. J. (2000) *Cell* **102,** 731–744.
6. Bertolotti, M., Abate, N., Loria, P., Dilengite, M., Carubbi, F., Pinetti, A., Digrisolo, A. & Carulli, N. (1991) *Hepatology* **14,** 830–837.
7. Otte, K., Kranz, H., Kober, I., Thompson, P., Hoefer, M., Haubold, B., Remmel, B., Voss, H., Kaiser, C., Albers, M., *et al.* (2003) *Mol. Cell. Biol.* **23,** 864–872.
8. Huber, R. M., Murphy, K., Miao, B., Link, J. R., Cunningham, M. R., Rupar, M. J., Gunyuzlu, P. L., Haws, T. F., Kassam, A., Powell, F., *et al.* (2002) *Gene* **290,** 35–43.
9. Willson, T. M., Jones, S. A., Moore, J. T. & Kliewer, S. A. (2001) *Med. Res. Rev.* **21,** 513–522.
10. Downes, M., Verdecia, M. A., Roecker, A. J., Hughes, R., Hogenesch, J. B., Kast-Woelbern, H. R., Bowman, M. E., Ferrer, J. L., Anisfeld, A. M., Edwards, P. A., *et al.* (2003) *Mol. Cell* **11,** 1079–1092.
11. Niesor, E. J., Flach, J., Lopes-Antoni, I., Perez, A. & Bentzen, C. L. (2001) *Curr. Pharm. Des.* **7,** 231–259.
12. Alberts, D. S., Hallum, A. V., III, Stratton-Custis, M., Garcia, D. J., Gleason-Guzman, M., Salmon, S. E., Santabarbara, P., Niesor, E. J., Floret, S. & Bentzen, C. L. (2001) *Clin. Cancer Res.* **7,** 1246–1250.
13. Walsh, D. T., Montero, R. M., Bresciani, L. G., Jen, A. Y., Leclercq, P. D., Saunders, D., EL-Amir, A. N., Gbadamoshi, L., Gentleman, S. M. & Jen, L. S. (2002) *Neurobiol. Dis.* **10,** 20–27.
14. Bishop-Bailey, D., Hla, T. & Warner, T. D. (2002) *Circ. Res.* **91,** 210–217.
15. Bishop-Bailey, D., Pepper, J. R., Larkin, S. W. & Mitchell, J. A. (1998) *Arterioscler. Thromb. Vasc. Biol.* **18,** 1655–1661.
16. Bishop-Bailey, D. & Hla, T. (1999) *J. Biol. Chem.* **274,** 17042–17048.
17. Urizar, N. L., Liverman, A. B., Dodds, D. T., Silva, F. V., Ordentlich, P., Yan, Y., Gonzalez, F. J., Heyman, R. A., Mangelsdorf, D. J. & Moore D. D. (2002) *Science* **296,** 1703–1706.
18. Cui, J., Huang, L., Zhao, A., Lew, J. L., Yu, J., Sahoo, S., Meinke, P. T., Royo, I., Pelaez, F. & Wright, S. D. (2003) *J. Biol. Chem.* **278,** 10214–10220.
19. Owsley, E. & Chiang, J. Y. (2003) *Biochem. Biophys. Res. Commun.* **304,** 191–195.
20. Ross, R. (1999) *N. Engl. J. Med.* **340,** 115–126.
21. Perez, A., Thuillard, J. L., Bentzen, C. L. & Niesor, E. J. (2003) *Cell Biol. Toxicol.* **19,** 95–105.
22. Seol, W., Choi, H. S. & Moore, D. D. (1996) *Science* **272,** 1336–1339.
23. Brendel, C., Schoonjans, K., Botrugno, O. A., Treuter, E. & Auwerx, J. (2002) *Mol. Endocrinol.* **16,** 2065–2076.
24. Borgius, L. J., Steffensen, K. R., Gustafsson, J. A. & Treuter, E. (2002) *J. Biol. Chem.* **277,** 49761–49766.
25. van Tol, A. (2002) *Curr. Opin. Lipidol.* **13,** 135–139.
26. Bishop-Bailey, D. & Wray, J. A. (2003) *Prostaglandins Other Lipid Mediat.* **71,** 1–22.
27. Lund, E. G., Menke, J. G. & Sparrow, C. P. (2003) *Arterioscler. Thromb. Vasc. Biol.* **23,** 1169–1177.
28. Howard, W. R., Pospisil, J. A., Njolito, E. & Noonan, D. J. (2000) *Toxicol. Appl. Pharmacol.* **163,** 195–202.
29. Nettles, K. W. & Greene, G. L. (2003) *Mol. Cell* **11,** 850–851.
30. Broughton, G., 2nd. (1994) *Am. J. Med. Sci.* **307,** 54–63.

PHARMACOLOGY